

# Shape effects on double beta decay of $^{70}\text{Zn}$ and $^{150}\text{Nd}$ in deformed shell model

R. Sahu<sup>1\*</sup> and V.K.B. Kota<sup>2,3</sup>

<sup>1</sup>*Physics Department, Berhampur University,  
Berhampur-760 007, Odisha, INDIA and*

<sup>2</sup>*Physical Research Laboratory, Ahmedabad - 380 009, INDIA*

<sup>3</sup>*Department of Physics, Laurentian University,  
Sudbury, ON P3E 2C6, CANADA*

## Abstract

Using deformed shell model based on Hartree-Fock intrinsic states with  $^{70}\text{Zn}$  as an example and employing two realistic effective interactions, namely jj44b that produces deformed shape and JUN45 that generates spherical shape, it is demonstrated that the  $0\nu$  and  $2\nu$  nuclear transition matrix elements for double beta decay will reduce considerably as we go from spherical shapes to deformed shapes. This result is further substantiated by using  $^{150}\text{Nd}$  as another example.

---

\*Electronic address: rankasahu@rediffmail.com

## I. INTRODUCTION

Double beta decay (DBD) is an important open problem of current interest. There are many experimental efforts [1–3] and also theoretical studies ( see for example [4, 5] and references cited therein) in particular for neutrinoless double beta decay. The nuclear transition matrix elements (NTME)  $M^{0\nu}$  for neutrinoless double beta decay ( $0\nu\beta\beta$ ) are found to vary considerably in different nuclear models. For example, QRPA values are always larger than the shell model values. Most variants of QRPA assume the nucleus to be spherical and hence they do not take into account the deformation of the nucleus. On the other hand, shell model takes into account all possible correlations, within the defined space, through the effective interaction. There are many studies which show that quadrupole deformation reduces the  $M^{0\nu}$ . Some of them are as follows. (i) energy density functional method including deformation and pairing fluctuations within the finite range density dependent Gogny force [6] where the authors show that deformation effects vary from 11% in  $^{82}\text{Se}$  to as high as 38% in  $^{128}\text{Te}$ . (ii) The proton-neutron QRPA with a realistic residual interaction [7]. (iii) Nuclear shell model [8] where a quadrupole-quadrupole term is added to the effective interaction and the deformation effects were studied by varying the strength of the quadrupole term. In addition, there is also an attempt to study the effect of hexadecapole deformation [9]. In this present report, we study the effect of changing from spherical to deformed shape on  $M^{0\nu}$  and  $2\nu$  half-lives, using realistic interactions within the deformed shell model (DSM) based on Hartree-Fock (HF) states. In the recent past, we have used DSM in the study DBD (both  $2\nu$  and  $0\nu$ ) in a number of nuclei in the  $A=60-90$  region [10–16].

In Section 2 we will discuss briefly the formulas for  $0\nu$  and  $2\nu$  half-lives and the DSM model. Sections 3 and 4 give the results obtained using spherical and deformed shapes for  $^{70}\text{Zn}$  and  $^{150}\text{Nd}$  nuclei respectively. Section 5 gives conclusions.

## II. DOUBLE BETA DECAY HALF-LIVES AND DEFORMED SHELL MODEL

Half-life for  $0\nu\text{DBD}$  for the  $0_i^+$  ground state (gs) of a initial even-even nucleus decaying to the  $0_f^+$  gs of the final even-even nucleus is given by [4]

$$[T_{1/2}^{0\nu}(0_i^+ \rightarrow 0_f^+)]^{-1} = G^{0\nu} (g_A)^4 |M^{0\nu}(0^+)|^2 \left( \frac{\langle m_\nu \rangle}{m_e} \right)^2, \quad (1)$$

where  $\langle m_\nu \rangle$  is the effective neutrino mass and  $G^{0\nu}$  is the phase space integral (kinematical factor). The NTME  $M^{0\nu}$  is essentially a sum of a Gamow-Teller like ( $M_{GT}$ ) and Fermi like ( $M_F$ ) two-body operators (we are neglecting other parts as in [15]). Then,

$$M^{0\nu}(0^+) = M_{GT}^{0\nu}(0^+) - \frac{g_V^2}{g_A^2} M_F^{0\nu}(0^+) = \langle 0_f^+ || \mathcal{O}(2 : 0\nu) || 0_i^+ \rangle. \quad (2)$$

As seen from Eq. (2),  $0\nu\text{DBD}$  half-lives are generated by the two-body transition operator  $\mathcal{O}(2 : 0\nu)$ . The  $g_A$  and  $g_V$  are the weak axial-vector and vector coupling constants. In our DSM analysis, we will use  $\mathcal{O}(2 : 0\nu)$  as given in [15, 16] and it contains the neutrino potential, Jastrow factor and a scale factor three. It is important to mention that the results in the present paper are independent of the scale factor used in [15, 16] as we are studying only the ratio of  $M^{0\nu}$  for spherical and deformed shapes. Eqs. (1) and (2) are a result of the closure approximation and this is justified *only if the exchange of the light Majorana neutrino is indeed the mechanism responsible for the  $0\nu\text{DBD}$ .*

For  $2\nu\text{DBD}$ , half-life for the  $0_I^+ \rightarrow 0_F^+$  decay is given by [19]

$$[T_{1/2}^{2\nu}]^{-1} = G_{2\nu} |M_{2\nu}|^2. \quad (3)$$

The kinematical factor  $G_{2\nu}$  is independent of nuclear structure and the  $M_{2\nu}$  is NTME given by,

$$M_{2\nu} = \sum_N \frac{\langle 0_F^+ || \sigma \tau^+ || 1_N^+ \rangle \langle 1_N^+ || \sigma \tau^+ || 0_I^+ \rangle}{[E_N - (E_I + E_F)/2] / m_e}. \quad (4)$$

Here,  $|0_I^+\rangle$ ,  $|0_F^+\rangle$  and  $|1_N^+\rangle$  are the initial, final and virtual intermediate states respectively and  $E_N$  are the energies of the intermediate nucleus. Similarly,  $E_I$  and  $E_F$  are the ground state energies of the parent and daughter nuclei (see [12, 15] for further details).

We will use DSM to calculate  $T_{1/2}^{2\nu}$  using the known values for  $G_{2\nu}$  and the NTME  $M^{0\nu}$  for nuclei with close to spherical shape and with deformation. In DSM, for a given nucleus, starting with a model space consisting of a given set of single particle (sp) orbitals and effective two-body Hamiltonian, the lowest energy intrinsic states are obtained by solving the

Hartree-Fock (HF) single particle equation self-consistently. Excited intrinsic configurations are obtained by making particle-hole excitations over the lowest intrinsic state. These intrinsic states do not have definite angular momenta and hence states of good angular momentum are projected from them. These good angular momentum states projected from different intrinsic states are not in general orthogonal to each other. Hence they are orthonormalized and then band mixing calculations are performed. DSM is well established to be a successful model for transitional nuclei (with  $A=60-90$ ) when sufficiently large number of intrinsic states are included in the band mixing calculations. For details see [15] and references therein.

### III. RESULTS FOR SPHERICAL AND DEFORMED SHAPES FOR $^{70}\text{Zn}$

In the DSM calculations for  $0\nu$  and  $2\nu$  NTME for  $^{70}\text{Zn}$ , used is the model space consisting of the orbitals  $^2p_{3/2}$ ,  $^1f_{5/2}$ ,  $^2p_{1/2}$  and  $^1g_{9/2}$  with  $^{56}\text{Ni}$  as the core. It is important to add that the same model space was used in many recent shell model and interacting boson model calculations [4, 17, 18] for  $^{76}\text{Ge}$  and  $^{82}\text{Se}$  nuclei and  $^{70}\text{Zn}$  is in the same region. Within this space we have employed two effective interactions. These are the *jj44b* interaction given in [20] with spherical single particle energies for the four orbits being  $-9.6566$ ,  $-9.2859$ ,  $-8.2695$  and  $-5.8944$  MeV respectively and the *JUN45* interaction given in [21] with spherical single particle energies for the four orbits being  $-9.8280$ ,  $-8.7087$ ,  $-7.8388$  and  $-6.2617$  MeV respectively. With these, we have first carried out axially symmetric HF calculations for the parent and the daughter nuclei  $^{70}\text{Zn}$  and  $^{70}\text{Ge}$  (for  $2\nu\text{DBD}$ , also for the intermediate odd-odd nucleus  $^{70}\text{Ga}$ ) for each of the two effective interactions.

The lowest energy HF solutions obtained using *jj44b* and *JUN45* interactions for  $^{70}\text{Zn}$  are shown in Fig. 1 and similarly for  $^{70}\text{Ge}$  in Fig. 2. It is clearly seen from the HF spectra in Figs. 1 and 2 that *jj44b* generates deformed solutions for the ground state of  $^{70}\text{Zn}$  and  $^{70}\text{Ge}$ . Note that the mass quadrupole moment given in the figure gives a measure of deformation. With *jj44b* interaction, the DSM calculated energy spectra for these two nuclei are compressed compared to the experimental spectrum. For example, for  $^{70}\text{Zn}$  the calculated  $E(2_1^+)$  is 0.355 MeV compared to the experimental value 0.885 MeV and similarly for  $^{70}\text{Ge}$  they are 0.64 MeV and 1.04 MeV respectively [16]. But, at the same time the calculated  $B(E2 : 2_1^+ \rightarrow 0_1^+)$  (14 W.u. and 18.8 W.u. for  $^{70}\text{Zn}$  and  $^{70}\text{Ga}$  respectively) are in close agreement with data

(16.5 W.u. and 20.9 W.u. respectively). These results are reported in [16]. On the other hand, as seen from Figs. 1 and 2, the JUN45 interaction generates nearly spherical solutions for these two nuclei. For this interaction, the spectrum is in close agreement with data but the  $B(E2 : 2_1^+ \rightarrow 0_1^+)$  is much smaller than data value; see Fig. 3. Both the calculated energy spectra and  $B(E2)$  values show that jj44b generates deformed shape and JUN45 generates spherical shape. Therefore, calculations of NTME for  $0\nu$  and  $2\nu$  using these interactions will give information about shape effects on NTME.

### A. $M^{0\nu}$ and $T_{1/2}^{2\nu}$ for $^{70}\text{Zn}$

In the DSM calculations of  $0\nu$  NTME using jj44b interaction, we have considered 30 lowest intrinsic states with  $K = 0^+$  for  $^{70}\text{Zn}$ , 26 lowest intrinsic configurations with  $K = 0^+$  for the daughter nucleus  $^{70}\text{Ge}$  (up to 6 MeV excitation in both nuclei) by making particle-hole excitations over the lowest HF intrinsic states generated for these nuclei. We project out  $0^+$  states from each of these intrinsic states and then perform band mixing calculations as discussed above. Similarly for JUN45 we have considered 81 lowest intrinsic states with  $K = 0^+$  for  $^{70}\text{Zn}$ , 68 lowest intrinsic configurations with  $K = 0^+$  for the daughter nucleus  $^{70}\text{Ge}$  (up to 5 MeV excitation in both nuclei) by making particle-hole excitations over the lowest HF intrinsic states generated for these nuclei. With jj44b interaction, the NTME  $M^{0\nu}$  comes out to be 2.13. However, for JUN45 interaction the value is 4.56. Thus we see a reduction by a factor 2 in  $M^{0\nu}$  as we go from spherical to deformed shape. Thus DSM is consistent with other theoretical calculations mentioned in Section 1. For further confirmation of this result we will turn  $2\nu$  NTME.

For  $2\nu$  DBD, firstly as discussed in [16],  $[E_N - (E_I + E_F)/2] = [1.1537 + E_{1+}]$  MeV and DSM is used to calculate  $E_{1+}$  for the intermediate nucleus  $^{70}\text{Ga}$  as well as the numerator in the sum in Eq. (4). In the DSM calculations using jj44b and JUN45 interactions, we have considered the same intrinsic states for  $^{70}\text{Zn}$  and  $^{70}\text{Ge}$  as in the calculation of  $0\nu$  NTME given above. In addition, for the intermediate nucleus  $^{70}\text{Ga}$ , 65 intrinsic states with  $K = 1^+$  or  $K = 0^+$  are used for jj44b interaction and 114 intrinsic states with JUN45 interaction. These are generated by making particle-hole excitations over the lowest HF intrinsic state generated for this nucleus. We project out  $1^+$  states from each of these intrinsic states and then perform a band mixing calculation as discussed above. Taking the phase space factor

$0.32 \times 10^{-21} \text{ yr}^{-1}$  given in [19], the DSM value for  $T_{1/2}^{2\nu}$  is  $3.39 \times 10^{23} \text{ yr}$  for jj44b interaction and  $4.94 \times 10^{22} \text{ yr}$  for JUN45 interaction. Thus, for  $2\nu$  DBD also the NTME (proportional to inverse of the half-life) is reduced by a factor of  $\sim 2.6$  as we go from spherical (JUN45) to deformed (jj44b) shape.

#### IV. RESULTS FOR SPHERICAL AND DEFORMED SHAPES FOR $^{150}\text{Nd}$

We then considered the double beta decay of  $^{150}\text{Nd}$  as another example. In the calculation of  $^{150}\text{Nd}$  and the daughter nucleus  $^{150}\text{Sm}$ , we used modified Kuo-Herling interaction [23] with a  $Z = 50$ ,  $N = 82$  core. The protons are in the  $^3s_{1/2}$ ,  $^2d_{3/2}$ ,  $^2d_{5/2}$ ,  $^1g_{7/2}$  and  $^1h_{11/2}$  orbits with spherical single particle energies -7.92783, -7.95519, -8.67553, -9.59581 and -6.83792 MeV, respectively. The neutrons are in the  $^3p_{1/2}$ ,  $^3p_{3/2}$ ,  $^2f_{5/2}$ ,  $^2f_{7/2}$ ,  $^1h_{9/2}$  and  $^1i_{13/2}$  orbits with spherical single particle energies for these orbits -1.050, -1.625, -1.964, -2.380, -0.895 and -0.261 MeV, respectively. The model space used here is same as in the recent interacting boson model calculations [4, 18]. As described before, we obtain the lowest energy HF configuration by solving the axially symmetric HF equation self-consistently. The lowest energy HF solutions for  $^{150}\text{Nd}$  and  $^{150}\text{Sm}$  obtained with this interaction are shown in figures 4 and 5. As seen from the quadrupole moments, both the nuclei have large deformations. To generate HF intrinsic states with nearly spherical shape, we artificially decreased the effective interaction to 1/10th of its value and perform axially symmetric HF calculation as described above. These nearly spherical HF single particle states are shown in figures 4 and 5. As expected, these two solutions have small quadrupole moment and hence small deformation. We then proceed to calculate  $0\nu$  NTME with the deformed and spherical solutions, separately. For the deformed solutions, we considered 38 intrinsic states with  $K = 0^+$  for  $^{150}\text{Nd}$ . Similarly we consider 17 intrinsic states with  $K = 0^+$  for the daughter nucleus  $^{150}\text{Sm}$ . Now, the NTME  $M^{0\nu}$  comes out to be 1.35. Then in the second case where we reduced the effective interaction matrix elements by a factor of 10, we considered 62 intrinsic states both for the parent and the daughter nuclei. The NTME  $M^{0\nu}$  comes out to be 3.06. Thus in this case also the  $0\nu$  nuclear matrix element increases by a factor of 2.33 as we go from deformed to spherical shape.

## V. CONCLUSIONS

We have demonstrated using DSM model and  $^{70}\text{Zn}$  as the example and employing two realistic effective interactions, namely jj44b that produces deformed shape and JUN45 that generates spherical shape, that the  $0\nu$  and  $2\nu$  NTME for double beta decay will reduce considerably as we go from spherical shapes to deformed shapes. This result is further confirmed by a calculation of  $0\nu$  NTME for  $^{150}\text{Nd}$ . Our results reported in this paper are an important addition, since the calculations are performed using two realistic interactions proposed for the same model space and DSM is transparent in determining shapes, to the existing analysis of deformation effects on NTME for DBD.

We would like to mention that since we have not included all the spin-orbit partners in the basis space, the Ikeda sum rule is not satisfied in our calculations. However, as mentioned before, many recent shell model and interacting boson model calculations [4, 17, 18] used the same model space. Violation of Ikeda sum rule may not be a serious deficiency in our calculations since we are only studying the change in double beta decay matrix elements with the change of nuclear shape. Calculations using much larger set of single particle orbits (these also need new effective interactions) are for future.

## Acknowledgments

RS is thankful to DST (Government of India) for financial support.

- 
- [1] A. Gando *et al.*, Phys. Rev. Lett. **110**, 062502 (2013).
  - [2] M. Auger *et al.*, Phys. Rev. Lett. **109**, 032505 (2012).
  - [3] M. Agostini *et al.*, Phys. Rev. Lett. **111**, 122503 (2013).
  - [4] J. Barea, J. Kotila, and F. Iachello, Phys. Rev. C **87**, 014315 (2013).
  - [5] J. Suhonen and O. Civitarese, J. Phys. G **39**, 124005 (2012).
  - [6] N.L. Vaquero, T.R. Rodriguez and J.L. Egido, Phys. Rev. Lett. **111**, 142501 (2013).
  - [7] D.L. Fang, A. Faessler, V. Rodin and F. Simkovic Phys. Rev. C **82**,051301(R) (2010).
  - [8] J. Menendez, A. Poves, E. Caurier and F. Nowacki, J. Phys.:Conference Series **267**, 012058 (2011).

- [9] R. Chandra, K. Chaturvedi, P.K. Rath, P.K. Raina and J.G. Hirsch, Eur. Phys. Lett. **86**, 32001 (2009).
- [10] R. Sahu, F. Šimkovic, and A. Faessler, J. Phys. G **25**, 1159 (1999).
- [11] S. Mishra, A. Shukla, R. Sahu, and V.K.B. Kota, Phys. Rev. C **78**, 024307 (2008).
- [12] A. Shukla, R. Sahu and V.K.B. Kota, Phys. Rev. C **80**, 057305 (2009).
- [13] R. Sahu and V.K.B. Kota, Int. J. Mod. Phys. E **20**, 1723 (2011).
- [14] R. Sahu, P.C. Srivastava and V.K.B. Kota, Can. J. Phys. **89**, 1101 (2011)
- [15] R. Sahu, P.C. Srivastava and V.K.B. Kota, J. Phys. G **40**, 095107 (2013)
- [16] R. Sahu and V.K.B. Kota, arXiv:1409.4929 [nucl-th]
- [17] R.A. Senkova and M. Horoi, Phys. Rev. C **90**, 051301 (2014); R.A. Senkov, M. Horoi and B.A. Brown, Phys. Rev. C **89**, 054304 (2014); D.L. Lincoln et al, Phys. Rev. Lett. **110**, 012501 (2013); J. Menendez, A. Poves, E. Caurier and F. Nowacki, Phys. Rev. C **80**, 048501 (2009); E. Caurier, J. Menendez, F. Nowacki and A. Poves, Phys. Rev. Lett. **100**, 052503 (2008).
- [18] J. Barea, J. Kotila, and F. Iachello, Phys. Rev. Lett. **109**, 042501 (2012); J. Barea and F. Iachello, Phys. Rev. C **79**, 044301 (2009).
- [19] F. Boehm and P. Vogel, *Physics of Massive Neutrinos* (Cambridge University Press, Cambridge, 1992).
- [20] B.A. Brown and A.F. Lisetskiy (unpublished); see also endnote (28) in B. Cheal *et al.*, Phys. Rev. Lett. **104**, 252502 (2010).
- [21] M. Honma, T. Otsuka, T. Mizusaki and M. Hjorth-Jensen, Phys. Rev. C **80**, 064323 (2009).
- [22] ENSDF Data Base, Brookhaven National Laboratory, USA, <http://www.nndc.bnl.gov/ensdf/index.jsp>.
- [23] W.T. Chou and E.K. Warburton, Phys. Rev. C **45**, 1720 (1992)



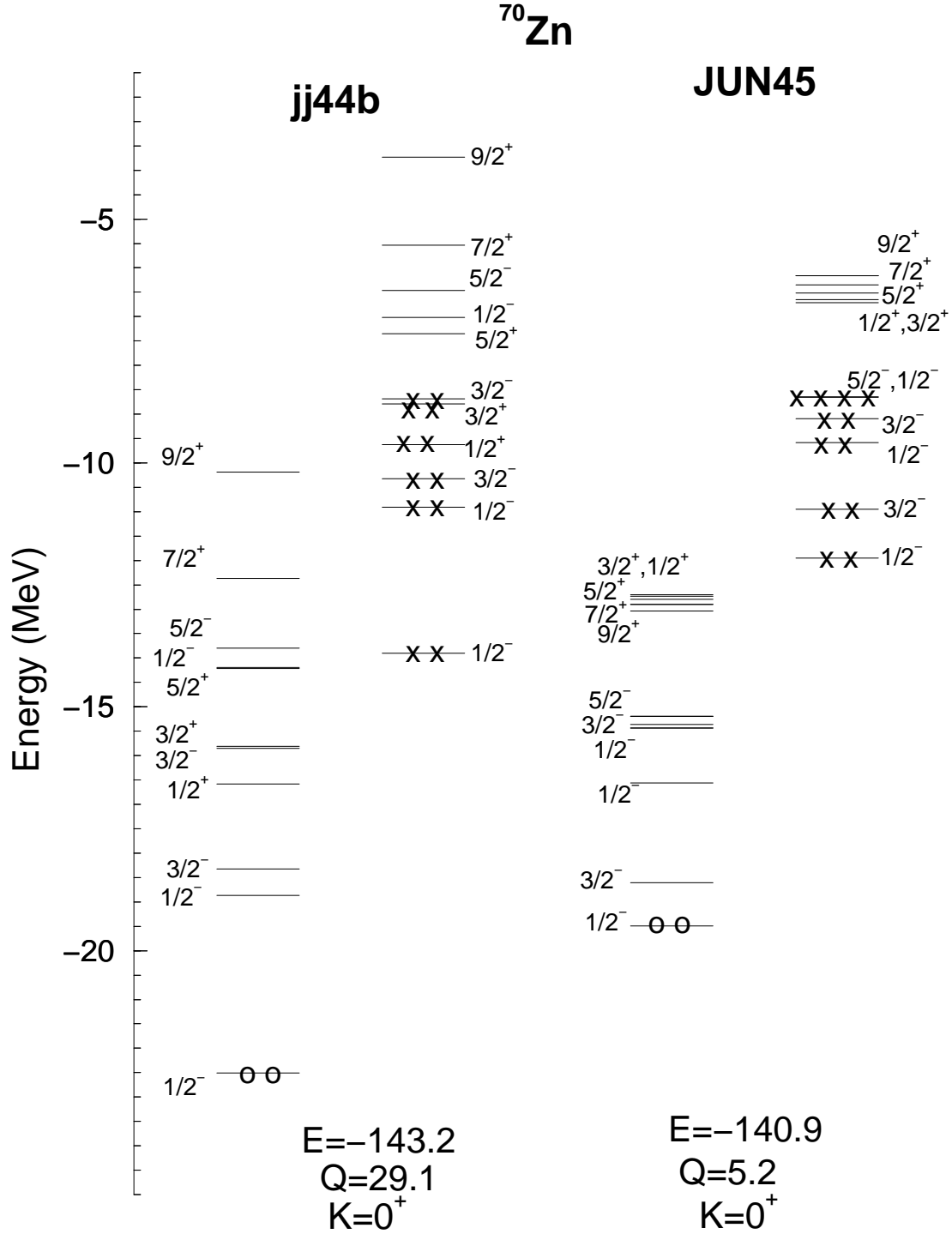


FIG. 1: HF single particle spectra for  $^{70}\text{Zn}$  corresponding to lowest prolate configurations generated by jj44b and JUN45 interactions. In the figures circles represent protons and crosses represent neutrons. The Hartree-Fock energy ( $E$ ) in MeV, mass quadrupole moment ( $Q$ ) in units of the square of the oscillator length parameter and the total  $K$  quantum number of the lowest intrinsic states are given in the figure. Each occupied single particle orbital is two fold degenerate because of time reversal symmetry.

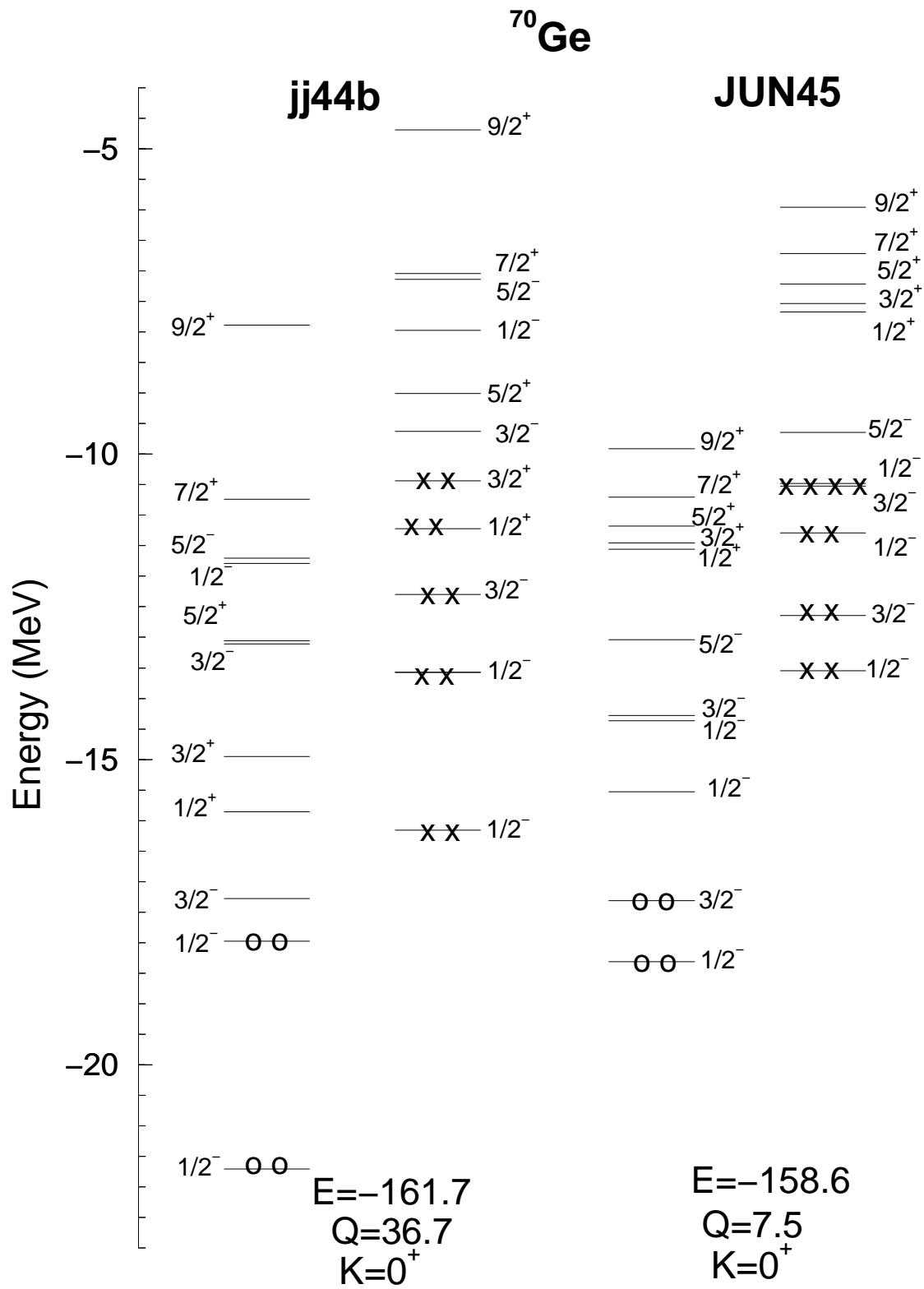


FIG. 2: Same as Fig. 1 but for  $^{70}\text{Ge}$ .

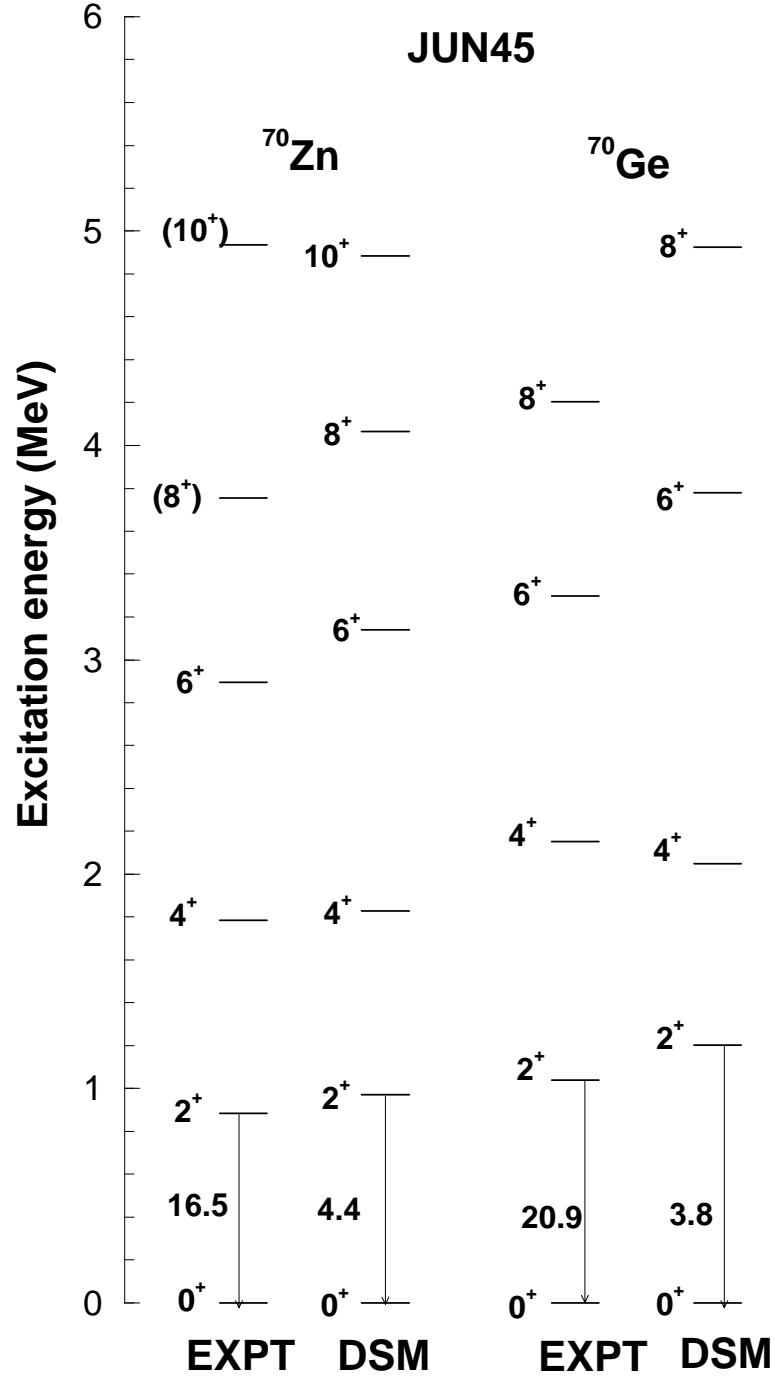


FIG. 3: The calculated yrast levels, using JUN45 interaction, for  $^{70}\text{Zn}$  and  $^{70}\text{Ge}$  compared with experiment. The experimental data are from ref [22]. The quantities near the arrows represent B(E2) values in W.u. and the effective charges used are same as in [16].

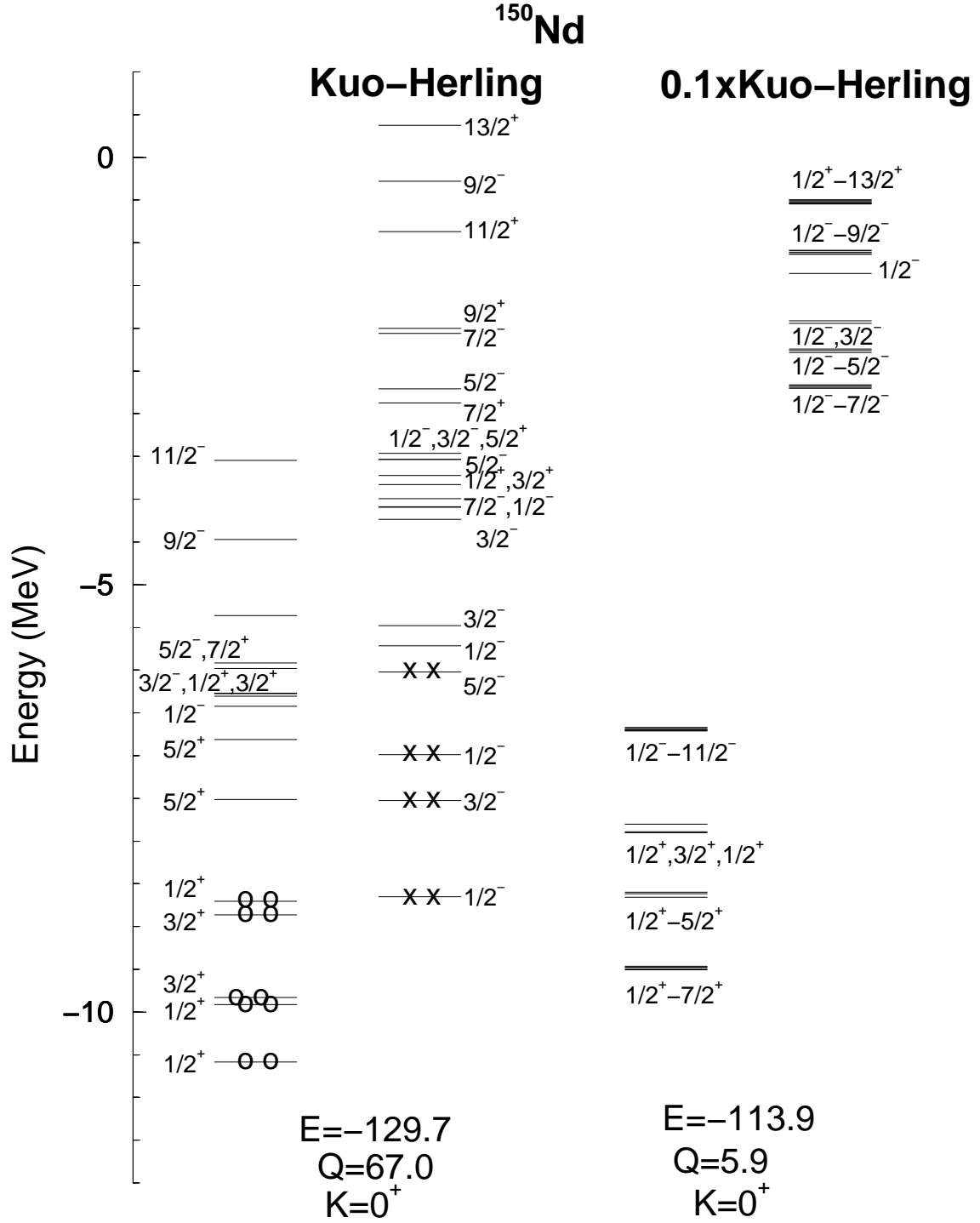


FIG. 4: Same as in Fig. 1 but for  $^{150}\text{Nd}$  with Kuo-Herling interaction (see text for details). In the spherical solution, the levels are degenerate as expected.

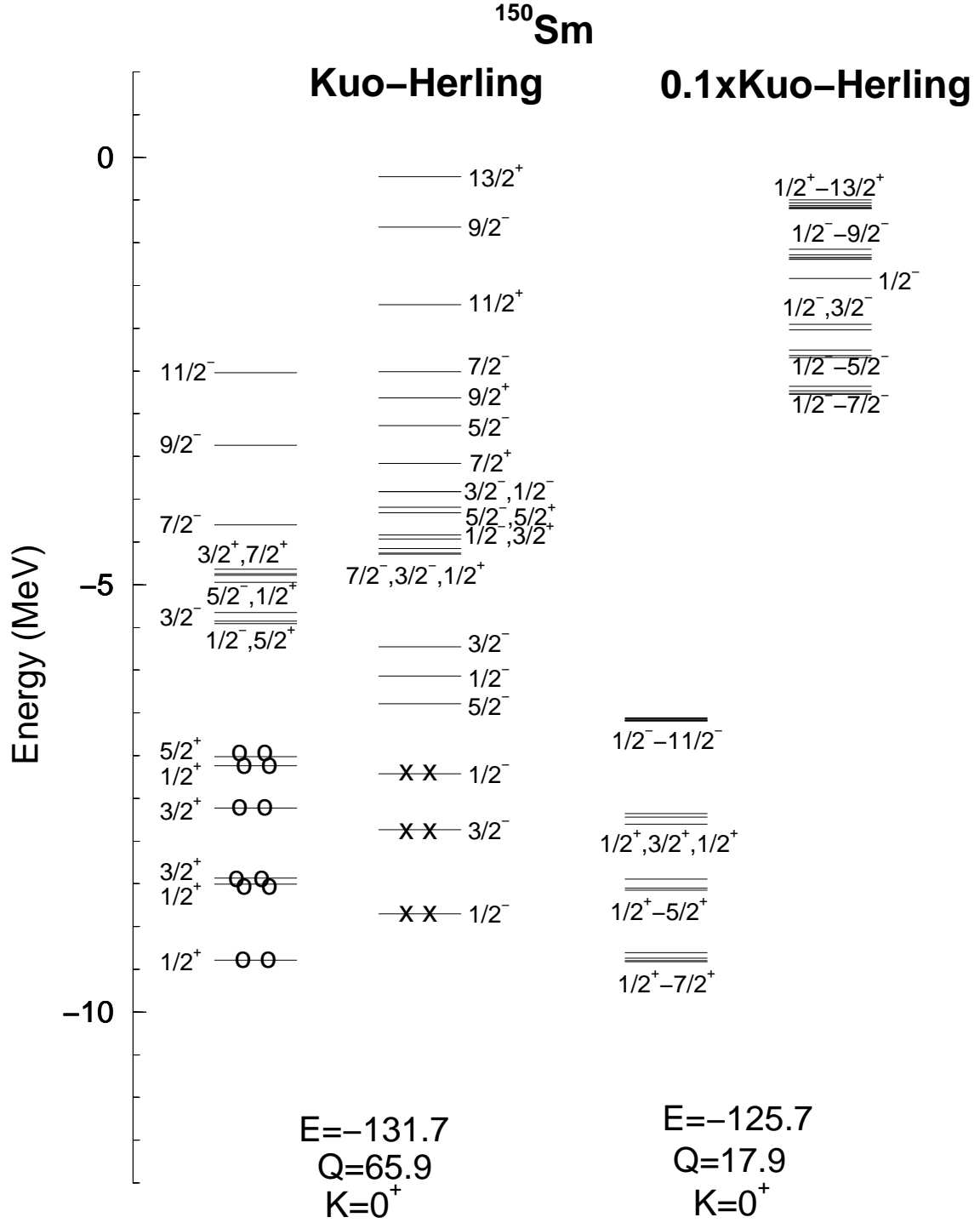


FIG. 5: Same as in Fig. 1 but for  $^{150}\text{Sm}$  with Kuo-Herling interaction (see text for details). In the spherical solution, the levels are degenerate as expected.